

Intrinsic Valence Band Study of Molecular-Beam-Epitaxy-Grown GaAs and GaN by High-Resolution Hard X-ray Photoemission Spectroscopy

Keisuke KOBAYASHI, Yasutaka TAKATA¹, Tetsuya YAMAMOTO², Jung-Jin KIM³, Hisao MAKINO⁴, Kenji TAMASAKU¹, Makina YABASHI, Daigo MIWA¹, Tetsuya ISHIKAWA¹, Shik SHIN¹ and Takafumi YAO^{3,4}

¹JASRI/SPring-8, 1-1-1 Kouto, Mikaduki-cho, Sayo-gun, Hyogo 679-5198, Japan

²RIKEN/SPring-8, 1-1-1 Kouto, Mikaduki-cho, Sayo-gun, Hyogo 679-5148, Japan

³Kochi University of Technology, 185 Miyanouchi, Tosayamada-cho, Kami-gun, Kochi 782-8502, Japan

⁴Research Center for Interdisciplinary Research, Tohoku University, Aramaki-Aoba, Aoba-ku, Sendai 980-8578, Japan

⁵Institute for Materials Research, Tohoku University, 2-1-1 Katahira, Aoba-ku, Sendai 980-8577, Japan

(Received April 26, 2004; accepted June 3, 2004; published July 16, 2004)

The electronic structures of molecular beam epitaxy (MBE)-grown GaAs and GaN have been studied by means of a technique using a newly developed surface-insensitive probe, namely, high-resolution hard X-ray (HX) synchrotron radiation ($h\nu = 5.95$ keV) photoemission spectroscopy (PES). The obtained valence band spectra and shallow core electronic states are compared with those calculated by the full-potential local density approximation (LDA) calculations explicitly including the Ga $3d$ core state. The experimental valence band spectra show a very good match with the calculations, simulated with linear combinations of the partial density of states. The Ga $3d$ core on d core states in GaN indicates a set of fine structures which are attributed to the Ga $3d$ -N $2s$ hybridization effect. The present experiments indicate that HX-PES provides an indispensable probe for investigating valence band electronic structures of materials, which has so far been impossible due to the limitations of proper surface preparation methods. [DOI: 10.1143/JJAP.43.L1029]

KEYWORDS: valence band, MBE, GaAs, GaN, X-ray photoemission spectroscopy, electronic structure, LDA calculation

We have recently succeeded in showing that intrinsic core and valence band (VB) photoemission (PES) in various materials is feasible utilizing high brilliance synchrotron radiation X-rays of 6 keV.^{1,2)} Surface cleaning procedures as well as the ultra high vacuum condition required to avoid sample surface contamination are verified to be unnecessary in this high energy region. This is in contrast to VB-PES in the VUV and soft X-ray region, which obviously remains surface sensitive even in the 0.8 keV photon energy regions.²⁾ The major benefits of this novel method are that enable us 1) to investigate valence band structures of materials which up to now has been impossible due to the lack of proper surface preparation methods, and 2) to obtain high-quality spectra in which degradation due to inelastic scattering is greatly reduced.²⁾

In this letter, we report on a quantitative analysis of the experimental valence band spectra with densities of states calculated using the local density approximation (LDA) in molecular beam epitaxy (MBE)-grown GaAs and GaN. The analysis yields relative values of the photoionization cross section, which indicate a strong solid-state effect. The hybridization of the shallow Ga $3d$ core states with N $2s$ is evidenced by structures in the N $2s$ -Ga $3d$ region in GaN, which are identified to be the bonding, nonbonding and antibonding states.

The samples were grown at Tohoku University by MBE, brought to SPring-8 in the ambient pressure without a capping layer, and introduced to the analysis chamber without any surface treatment prior to the measurements. Measurements were performed at BL29XU, an X-ray undulator beam line of SPring-8. The X-rays were monochromatized with a Si 111 double-crystal monochromator. The energy bandwidth was reduced by a channel-cut monochromator with Si 333 reflection. Photon flux was 2×10^{11} counts/s in a focal spot of $0.12 \text{ mm} \times 0.7 \text{ mm}$ at the sample position at 5.95 keV with a bandwidth of 70 meV. Gammatdata Scienta SES2002, modified to measure kinetic energies up to 6 keV, was used as an electron analyzer. Total

instrumental energy resolution was 240 meV at a path energy of 200 eV. Experiments were performed under a pressure of 10^{-5} – 10^{-6} Pa at room temperature and 10^{-8} Pa at 40 K. The electronic band structure calculations were based on the local-density approximation treatment of electronic exchange and correlation^{3–6)} and on the augmented spherical wave (ASW) formalism for the solution of effective single-particle equations.⁶⁾ The atomic sphere approximation (ASA) with a correction term was adopted. For valence electrons, we employed $3d$, $4s$ and $4p$ orbitals for Ga, outermost s and p orbitals for N atoms and outermost s , p and d orbitals for As atoms. Brillouin zone integration was carried out for 4.5×10^4 points in an irreducible wedge.

The thick solid curve in Fig. 1 is the GaAs valence band spectrum at 40 K. As shown by the broken curve, the background of the spectrum is weak and almost linear. The thin solid curve is the energy distribution curve (EDC) of the

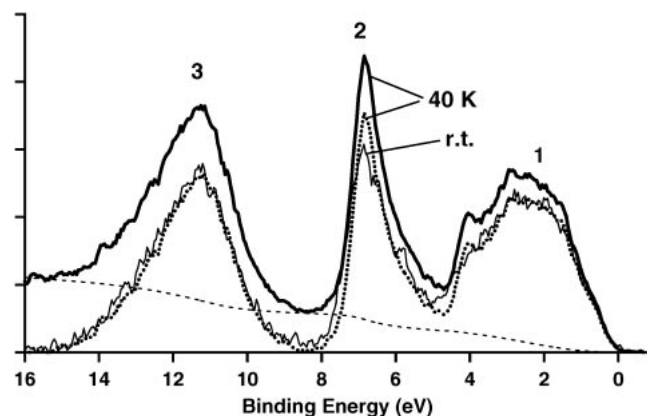


Fig. 1. Bold solid curve shows experimental raw spectrum of GaAs valence band at 5.95 keV photon energy at 40 K. Bold dotted curve is photoelectron energy distribution curve (EDC), which is obtained by subtracting the background (shown by thin dashed curve) from the raw spectrum. Thin solid curve shows EDC of the same sample at room temperature.

valence band photoelectrons at 40 K, which is obtained by subtracting the backgrounds from the experimental spectrum. The dotted curve is the EDC at room temperature obtained by the same background subtracting procedure. It should be noted that the band denoted by 2 (predominantly the Ga 4*s*-As 4*p* mixed band) shows a sharp singular feature, as seen in the calculated density of states.⁷⁾ The feature is more prominent at lower temperature, giving evidence that phonon scattering decreases at low temperature. Band 3, which is the mainly As 4*s*-like band, exhibits significant broadening compared with that in the LDA calculation. The experimental width of this band is almost unchanged on lowering the temperature. This suggests that the main contribution is from lifetime broadening caused by radiative recombination and Auger decay of the holes with electrons in band 1 (dominated by As 4*p*, as shown in Fig. 2(a)).

Figure 2(a) shows total density of state (DOS) obtained by the LDA calculation for GaAs. The contribution from each partial density of states is indicated by different filling patterns. The thin solid curve in Fig. 2(b) is the least-squares-fitted calculated EDC defined as $EDC(E) = \sum a(i)DOS_i(E)$, where $DOS_i(E)$ is the partial density of the *i*-th partial state and $a(i)$ is the fitting parameter. Again, contributions from partial states are shown by the filling patterns. In this fitting procedure, first the experimental EDC is shifted to match the valence band top with that of calculated EDC. Then the parameter $a(i)$ is determined such that the sum of the square of the deviation from the experimental EDC becomes minimum for bands 1 and 2. The fit accuracy, estimated as the ratio of square root of the sum of the square deviation to the sum of the calculated EDC values is 3.4%. Significant lifetime broadening of band 3, and large shift of Ga 3*d* prevent adoption of the same method as used for bands 1 and 2. Thus we minimize the differences between integrated areas of the calculated and experimental EDCs for these states. The resultant differences of the integrated areas are 0.2% and 5%, for band 3 and Ga 3*d* states, respectively. The EDC resembles the calculated bare total DOS in shape in the valence band region. The As 4*s* partial DOS contribution is slightly stronger in the EDC than in the DOS. The peak positions of

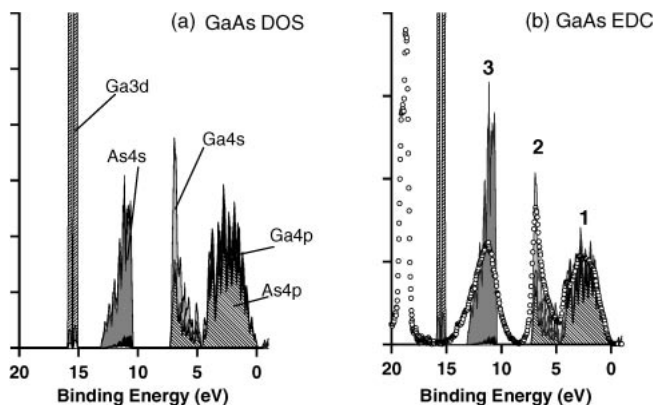


Fig. 2. (a) Calculated total and partial DOSs of GaAs. (b) Comparison between experimental and calculated EDCs for GaAs. Curve fitting is done by least-mean-squares method with linear combination of partial DOS contributions. Contribution from each partial density of state is distinguished by different filling patterns in both (a) and (b).

bands 1 and 2 coincide well, but band 3 of the experimental EDC shifts by about 0.3 eV toward a lower binding energy. Ga 3*d*, which shows atom like spin-orbit splitting of 0.45 eV, appears at about 3.5 eV deeper binding energy than that in the calculation. This difference in energy position is well known to be due to the defect in the LDA calculation when used to predict binding energies of shallow core states.⁷⁾

The LDA calculated total and partial DOS, experimental EDC, and the curve-fitting result for GaN are shown in Figs. 3(a) and 3(b) in the same manner as in Fig. 2 for GaAs. In this case, differences between integrated areas of the calculated and experimental N 2*s* and Ga 3*d* structures are minimized. The resultant accuracies are 1.5%, 5% and 0.8%, for bands 1 and 2, N 2*s* and Ga 3*d* areas, respectively. The EDC shape is significantly different from that of the bare total DOS, however, a curve fitting using a linear combination of partial DOS is again successful. It should be noted that Ga 4*s* is the dominant contribution to the EDC in this case. This is in contrast to the case of GaAs where all the valence orbitals contribute almost equally to the EDC. The Ga 3*d* peak shows a broadened shape in Fig. 3(b). This is due to the hybridization between Ga 3*d* and N 2*s*.⁸⁻¹⁰⁾ Interesting point is that fine structures are recognizable as shown by the vertical bars in the inset of the same figure. The dotted curve in the inset shows the first derivative spectrum. This characteristic feature of the Ga 3*d* band due to hybridization with N 2*s* is clearly reproduced in the results of the LDA calculation, although the calculated structures appear at the lower binding energy. A simple Ga 3*d*-N 2*s* hybridization model leads to the following interpretation. In the tetrahedral crystal field, the Ga 3*d* level degeneracy is lifted and splits into t_2 and e states. The small Ga 3*d*-N 2*s* energy separation gives rise to hybridization between Ga 3*d* and N 2*s*. The hybridization causes splitting of the t_2 state into bonding (t_{2g}) and antibonding (t_{2u}), states, while the

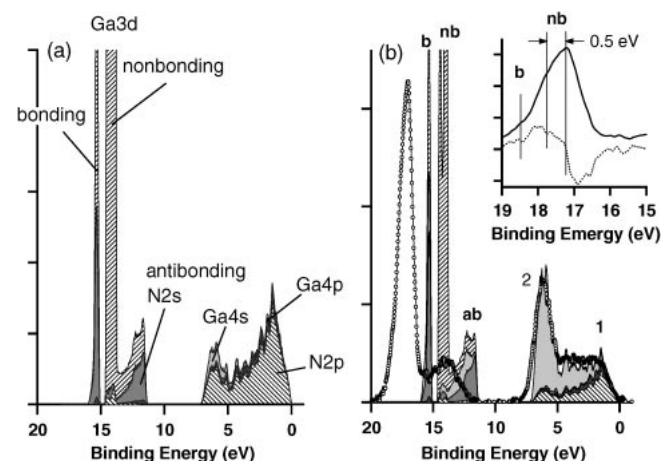


Fig. 3. (a) Calculated total and partial density of states of GaN. The hybridization is evident in the Ga 3*d*-N 2*s* binding energy region. (b) Calculated and experimental EDCs. Background of the experimental data was almost linear, and at 20 eV, it is 6% of the Ga 3*d* peak heights of GaN. The bonding, nonbonding, and antibonding features formed due to hybridization between Ga 3*d* and N 2*s* are distinguishable in the enlarged experimental spectrum shown in the inset and are denoted by b, nb, and ab, respectively. Note that spin-orbit splitting is observed in the experimental nb band even though it is smeared by broadening due to lifetime broadening.

Table I. Relative subshell photoionization cross section.

	cation <i>s</i>	cation <i>p</i>	anion <i>s</i>	anion <i>p</i>
GaAs	0.348 (1.18)	0.282	1.115 (2.4)	0.782
GaN	0.748 (1.18)	0.083	0.285 (0.3)	0.232 (0.032)

The relative photoionization cross sections of valence band partial states in GaAs and GaN, normalized to those of cation *3d* state. Cross sections for these two compounds are smaller than atomic values, which were obtained using interpolated values of atomic calculations in the photon energy region from 21 eV to 8 keV, are shown in parentheses.

nonbonding state e_g remains nearly atomic, showing spin-orbit splitting. The bonding t_{2g} state is mainly Ga *3d*-like; whereas the antibonding t_{2u} state is N *2s* dominated. The bonding t_{2g} state is recognized at 18.47 eV in the experimental EDC.

The nonbonding e_g state remains almost atom-like, and shows spin-orbit splitting of about 0.5 eV. Corresponding identification of the experimental Ga *3d* structures is shown in Fig. 3(a). In the case of GaAs, hybridization of Ga *3d* is negligible due to the larger energy separation between Ga *3d* and As *4s*, resulting in a well-resolved atom-like spin-orbit doublet in both the experimental and the calculated spectrum.

The photoionization cross section $\sigma(i)$ of the *i*-th subshell is expressed as $\sigma(i) = A \int a(i) \text{DOS}(i) dE$. It is not possible to estimate absolute values of $\sigma(i)$ from the curve fitting in these experiments, because of uncertainties in parameter *A*, which includes unknown factors such as photon flux, acceptance, transmission, and the detection efficiency of analyzer. Thus we define relative photoionization cross sections by $\sigma^*(i) = \sigma(i)/\sigma(\text{Ga } 3d)$. The $\sigma^*(i)$ values are summarized in Table I along with relative atomic photoionization cross sections also normalized at the atomic Ga *3d* cross section.¹¹⁾ The relative cross sections of valence orbitals in both GaAs and GaN are significantly smaller than those of corresponding atomic subshells. In the case of GaN, the Ga *4s* relative cross section is about one order of magnitude larger than that of Ga *4p* and about three times larger than that of N *2s*. The N *2p* contribution is negligible. This causes dissimilarity of the EDC from the bare total DOS, as seen in Figs. 3(a) and 3(b). It is noted that the values in GaN are closer to atomic values than those in GaAs. This may be related to less hybridization between cations and anions in GaN than in GaAs. To understand this solid-state effect, we must carry out a set of experimental studies of compounds with a systematic variation of cations and anions.

In conclusion, we have performed high-resolution hard X-ray photoemission spectroscopy (HX-PES) of valence band structures in GaAs and GaN, utilizing high-brilliance X-ray undulator radiation at SPring-8. Measurements of throughput sufficiently high for practical use was realized with total resolution of around 250 meV. The high quality of the obtained spectra allows a quantitative analysis by means of an LDA calculation, yielding relative photoionization cross sections of the valence orbitals. The results indicate the strong modification of the photoionization cross section. It has been found that the Ga *3d*-N *2s* hybridization is reflected in the Ga *3d* lineshape, in which bonding and spin-orbit split nonbonding Ga *3d* states are recognized for the first time. The present experiments clearly confirm the “surface free” and “inelastic scattering free” characteristics of HX-PES, and are expected to allow us to apply HX-PES to a wide range of materials including thin films, buried layers, nanoparticles, liquids, and organic and biomaterials, for the precise investigation of valence band structures as well as chemical state analysis using core level spectroscopy. The feasibility of HX-PES has already been examined for various types of materials, and reports are under preparation for publication.

We are thankful to Dr. J. H. Chang, Dr. P. P. Chen, and Dr. H. J. Ko for providing epitaxial samples. We are also grateful to Dr. T. Tokushima for his assistance during the experiments. Dr. A. Chainani is much appreciated for valuable discussion and critical reading of the manuscript.

- 1) K. Kobayashi, M. Yabashi, Y. Takata, T. Tokushima, S. Shin, K. Tamasaku, D. Miwa, T. Ishikawa, H. Nohora, T. Hattori, Y. Sugita, O. Nakatsuka, A. Sakai and S. Zaima: *Appl. Phys. Lett.* **83** (2003) 1005.
- 2) Y. Takata, K. Tamasaku, T. Tokushima, D. Miwa, A. Shin, T. Ishikawa, M. Yabashi, K. Kobayashi, J. J. Kim, T. Yao, T. Yamamoto, M. Arita, H. Namatame and M. Taniguchi: *Appl. Phys. Lett.* **84** (2004) 4310.
- 3) W. Kohn and L. J. Sham: *Phys. Rev.* **140** (1965) A1133.
- 4) L. Hedin and B. I. Lundquist: *J. Phys. C* **4** (1971) 3107.
- 5) U. von Barth and L. Hedin: *J. Phys. C* **5** (1972) 1629.
- 6) A. R. Williams, J. Kübler and C. D. Gelatt: *Phys. Rev. B* **19** (1979) 6094.
- 7) W. R. L. Lambrecht and B. Segall: *Phys. Rev. B* **50** (1994) 14155.
- 8) C. B. Stagescu, L. C. Duda, K. E. Smith, J. H. Guo, J. Nordgren, R. Singh and T. T. Moustakas: *Phys. Rev. B* **54** (1996) R17335.
- 9) L. C. Duda, C. Stagescu, J. Downes, K. E. Smith, D. Korakakis, T. D. Moustakas, J. Guo and J. Nordgren: *Phys. Rev. B* **58** (1998) 1928.
- 10) P. Ryan, C. McGuinness, J. E. Downes, K. E. Smith, D. Doppalapudi and T. D. Moustakas: *Phys. Rev. B* **65** (2002) 205201.
- 11) J. J. Yeh and I. Lindau: *Atomic Data & Nuclear Data Tables* **32** (1985) 1.